# Warming, acidification, and calcification feedback during the first hyperthermal of the Cenozoic – the Latest Danian Event

Margareta Harbich[1], James S.K. Barnet[2], James W.B. Rae[2], and Dick Kroon[1]

[1]*School of GeoSciences, University of Edinburgh, Edinburgh, UK*

[2]*School of Earth & Environmental Sciences, University of St Andrews, St Andrews, UK*

## ABSTRACT

The Latest Danian Event (LDE; ~62.15 Ma) is a major double-spiked eccentricity-driven transient warming event and carbon cycle perturbation (hyperthermal) in the early Paleocene, which has received significantly less attention compared to the larger events of the late Paleocene–early Eocene. A better understanding of the nature of the LDE may broaden our understanding of hyperthermals more generally and improve our knowledge of Earth system responses to extreme climate states. Here we present planktic and benthic foraminiferal Mg/Ca and B/Ca records that shed new light on changes in South Atlantic temperature and carbonate chemistry during the LDE. Our planktic Mg/Ca record reveals a pulsed increase in sea surface temperature of at least ~1.5°C during the older carbon isotope excursion, and ~0.5°C during the younger isotope excursion. We observe drops in planktic and benthic B/Ca, synchronous with pronounced negative excursions in benthic $\delta^{13}C$, which suggest a shift in the carbonate system towards more acidic, dissolved inorganic carbon-rich conditions, in both the surface and deep ocean. Conditions remain more acidic following the LDE, which we suggest may be linked to an enhanced ocean alkalinity sink due to changes in the make-up of planktic calcifiers, hinting at a novel feedback between calcifier ecology and ocean-atmosphere $CO_2$.

## INTRODUCTION

The warmhouse climate of the early Paleogene is punctuated by several geologically brief (< 200,000 years) warming events termed 'hyperthermals' (e.g., Zachos et al., 2010; Barnet et al., 2019). The Latest Danian Event (LDE; ~62.15 Ma), the first major hyperthermal of the Paleocene, was first described by Bornemann et al. (2009) in sediments from the southern Tethys shelf on the basis of distinct negative excursions in benthic foraminiferal $\delta^{13}C$, as well as lithological and biostratigraphical observations. It was also identified by Westerhold et al. (2008) in detailed cyclostratigraphic and XRF core scanning data by the alternative name "Top Chron27n". The event has more recently been identified in well-resolved marine sequences globally based on the coincidence of pronounced twinned negative excursions in benthic foraminiferal $\delta^{13}C$ and $\delta^{18}O$ with two 100-kyr eccentricity maxima (Barnet et al., 2019; Figure 1A, 2A). These excursions suggest a pulsed injection of large quantities of isotopically light carbon to the ocean-atmosphere system and coincident deep-sea warming of between 1–3 °C, thought to be triggered by intensified summer insolation (e.g., Bornemann et al., 2009; Westerhold et al., 2011; Jehle et al., 2015; Alegret et al., 2016; Deprez et al., 2016; Barnet et al., 2019; Jehle et al., 2019). Peaks in Fe intensity and minima in $CaCO_3$ content during this interval (Figure 1C, 3D) suggest that this carbon release also caused deep-sea carbonate dissolution (e.g., Westerhold et al., 2008; Jehle et al., 2019).

While the LDE is well-documented in stable isotope records, relatively little is known about changes in ocean temperature and carbonate chemistry across the event compared to the larger, better-studied hyperthermals of the late Paleocene–early Eocene. The foraminiferal Mg/Ca and B/Ca proxies have been applied to the Paleocene-Eocene Thermal Maximum (PETM) to reconstruct changes in temperature and carbonate chemistry (e.g., Babila et al., 2018; Barnet et al., 2020; Haynes and Hönisch, 2020). Here we present the first paired B/Ca and Mg/Ca records for the LDE interval to shed light on the evolution of carbonate chemistry in the surface and deep ocean and better constrain the magnitude of sea-surface warming.

## MATERIALS AND METHODS

This study uses samples from a stratigraphically continuous section of Paleocene clay-rich nannofossil ooze, recovered from Ocean Drilling Program (ODP) Site 1262 (Walvis Ridge, South Atlantic, 27°11.15′S, 1°34.62′E, 4759 m depth at present-day, ~3000–3500 m paleodepth for the studied time interval; Zachos et al., 2004). The samples are calibrated to the age model of Barnet et al. (2019), which has been orbitally tuned to the La2010b orbital solution of Laskar et al. (2011) based on the recognition and counting of the stable 405-kyr eccentricity cycle in the high-resolution benthic $\delta^{13}C$ dataset from this site.

We generated planktic trace element records using the mixed-layer planktic species *Morozovella conicotruncata* and *M. angulata*, and benthic trace element records using the epifaunal benthic species *Nuttallides truempyi* and *Stensioeina beccariiformis*. The samples were oxidatively cleaned and analysed by ICPMS, with average analytical error (2SD) of 3% and 2% for *N. truempyi* and *S. beccariiformis* B/Ca, respectively; and 2% for planktic B/Ca and Mg/Ca (see Supplementary Information). We assessed potential clay contamination using Al/Ca ratios, excluding two anomalous planktic samples with elevated Al/Ca from our final dataset. We assessed the degree of foraminiferal preservation using SEM imagery and a linear cross plot of Mg/Ca and Sr/Ca ratios, and observe no evidence for the overprinting of Mg/Ca by diagenetic recrystallization (see Supplementary Information).

To reconstruct surface ocean carbonate chemistry, the ratio of borate ion to dissolved inorganic carbon ($[B(OH)_4^-]$/DIC) was calculated from planktic B/Ca values using the "Low-DIC" calibration of Haynes et al. (2019). This calibration is based on several modern planktic species that were cultured under simulated early Cenozoic seawater conditions and was chosen in favour of the "High pH" calibration since early Paleocene pH is thought to have been relatively low, at around ~7.8 (Zeebe and Tyrrell, 2019; Henehan et al., 2019; Rae et al., 2021).

Changes in deep-sea carbonate saturation state ($\Delta\Delta[CO_3^{2-}]$) were calculated from the *N. truempyi* B/Ca data using the species-specific calibration equation of Brown et al. (2011) for *N. umbonifera*, the closest extant relative of *N. truempyi*. We followed modifications given in Kender et al. (2014) to account for differences in the boron concentration of Paleogene seawater compared to the modern day.

For sea surface temperature (SST) reconstruction, we followed recommendations given in Hollis et al. (2019) – see Supplementary Information. Our raw planktic Mg/Ca data were first corrected to a pH estimate of 7.77 based on modelling studies (Zeebe & Tyrrell, 2019; as pH reconstructions at this time are sparse), using the linear correction of Evans et al. (2016a). Seawater Mg/Ca for the LDE interval was estimated from published values based on well-preserved corals (Gothmann et al., 2015). We do not correct our Mg/Ca values for changes in salinity, as we assume the impact on Mg/Ca of the likely range in salinity at this open ocean site to be negligible. Given the uncertainties in factors controlling absolute temperature estimates from Mg/Ca in this time interval (e.g. seawater Mg/Ca), our main figures plot relative temperature change, which is likely to be more robust than the absolute values.

## RESULTS

Our benthic B/Ca data display negative excursions broadly coincident with the double-spiked negative benthic carbon and oxygen isotope excursions defining the LDE at ~62.1 and ~62.0 Ma (Figures 1 and 2). *N. truempyi* B/Ca drops during both the oldest negative carbon isotope excursion (LDE1) and the second, younger CIE (LDE2; Figure 1F). These shifts correspond to to ~7 and ~5 umol/kg decreases in carbonate ion concentration $\Delta[CO_3^2]$ during LDE1 and LDE2, respectively (Figure 1G). LDE1 is also captured in the *S. beccariiformis* dataset (Figure 1F), with limited data resolution preventing detection of the second event.

Our planktic data show a decrease in B/Ca and $[B(OH)_4^-]$/DIC across the LDE, with a notable drop in LDE2, and a less well-defined LDE1 (due to scarcity of planktic foraminifera) which appears to lag the onset of the LDE1 event as recorded by benthic $\delta^{13}C$ (Figure 1D and 1E). We observe pulsed increases in Mg/Ca and SST at LDE1 and LDE2, with peaks of ~1.5°C compared to pre-event conditions (Figure 2C and D). These occur at times of notable deep ocean warming of ~2.5°C recorded in benthic $\delta^{18}O$ (Figure 2B), although

the planktic SST maxima at LDE1 lags the benthic $\delta^{18}O$ excursion. We also note that recovery of planktic and benthic B/Ca following the LDE is limited, suggesting a shift to more acidic state of the ocean carbonate system.

## DISCUSSION

### Ocean Warming

Our reconstructed temperature change may suggest that warming during the LDE interval at ODP Site 1262 was stronger in the deep sea than at the surface. Climate model outputs for other hyperthermals during the late Paleocene–early Eocene interval suggest enhanced warming in the polar regions compared to low latitudes (e.g., Evans et al., 2018; Inglis et al., 2020). Given that the deep waters bathing ODP Site 1262 during this time were likely sourced from the Southern Ocean, a greater magnitude of deep sea warming at this site is not unlikely. However, $\delta^{18}O$ measured in both *Morozovella* spp. and *N. truempyi* at ODP Site 1262 by Jehle et al. (2019) show similar changes across the LDE interval, so we caution that additional influences on one or both of Mg/Ca and $\delta^{18}O$ may need to be accounted for to allow their direct comparison in terms of temperature change. We also note that the resolution of our planktic trace element record across the LDE1 peak is insufficient to fully resolve the surface ocean warming at the onset of this event. Sediment reworking could potentially explain the lag in our planktic record at the LDE1 peak and may impact *Morozovella* spp. more than benthics due to the increase in *Morozovella* abundance over the LDE (e.g. Jehle et al., 2019). There may also be undetected changes occurring below our sampling resolution, perhaps driven by precession, or other competing influences, such as changes in stratification, which could influence the regional surface expression of warming at ODP Site 1262 (Jehle et al., 2019).

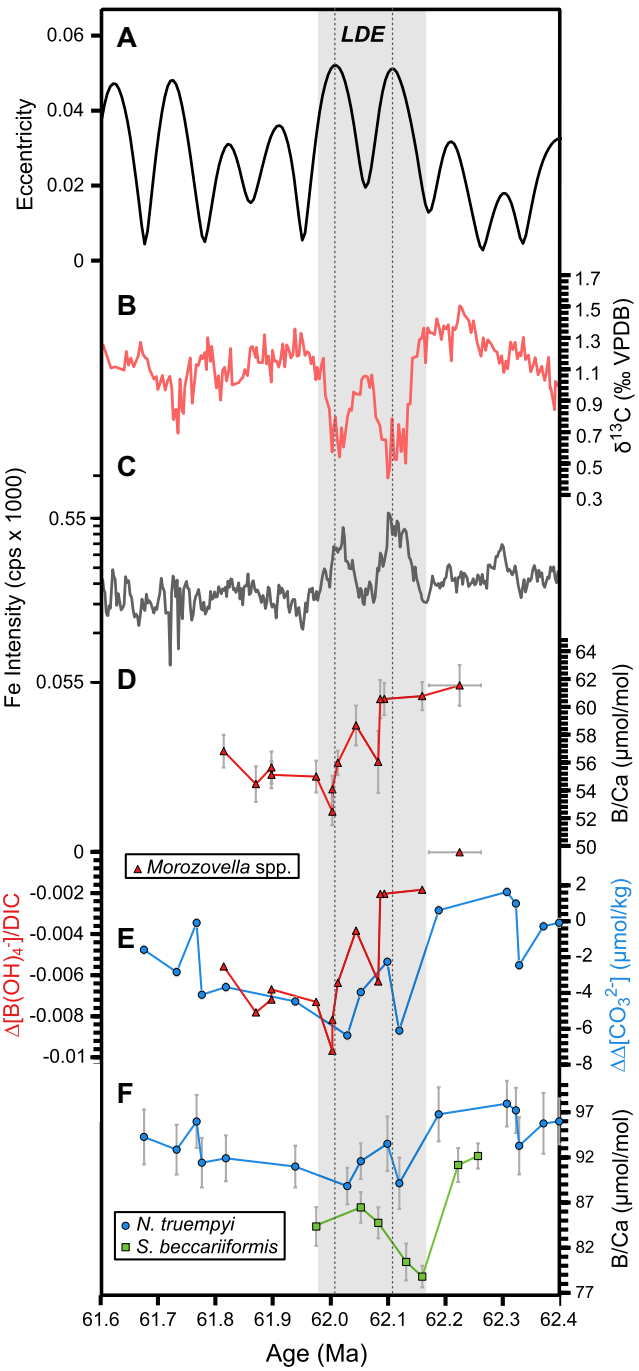


Figure 1: Changes in carbonate chemistry across the LDE at ODP Site 1262. Dashed vertical lines indicate the two benthic $\delta^{13}C$ excursions forced by two 100-kyr eccentricity maxima, whilst the vertical grey bar encompasses the LDE as a whole. A: La2010b orbital solution of Laskar et al. (2011), labelled with the LDE interval. B: Benthic foraminiferal $\delta^{13}C$ record (Barnet et al., 2019). C: Fe intensity record (Westerhold et al., 2008). D: Planktic B/Ca ratios of Morozovella spp. (this study). E: Planktic borate/dissolved inorganic carbon ($[B(OH)_4^-]/DIC$) ratios of Morozovella spp. (red triangles, this study) and change in benthic carbonate ion saturation ($\Delta\Delta[CO_3^{2-}]$) from B/Ca in N. truempyi (blue dots, this study). F: Benthic B/Ca ratios of Nuttallides truempyi (blue dots; this study) and Stensioeina beccariiformis (green squares; this study. Average propagated analytical uncertainty associated with the B/Ca data for ($[B(OH)_4^-]/DIC$) and ($\Delta[CO_3^{2-}]$) is ±0.0001 and ±0.21 µmol/kg, respectively.

### Deep Sea Dissolution

Our new trace element data show a clear response of the carbonate system to an injection of isotopically light carbon to the ocean-atmosphere system during the LDE. The observed coeval decreases in benthic B/Ca and $\Delta[CO_3^{2-}]$ in both *N. truempyi* and *S. beccariiformis* are synchronous with the negative benthic CIE measured at ODP Site 1262 (Figure

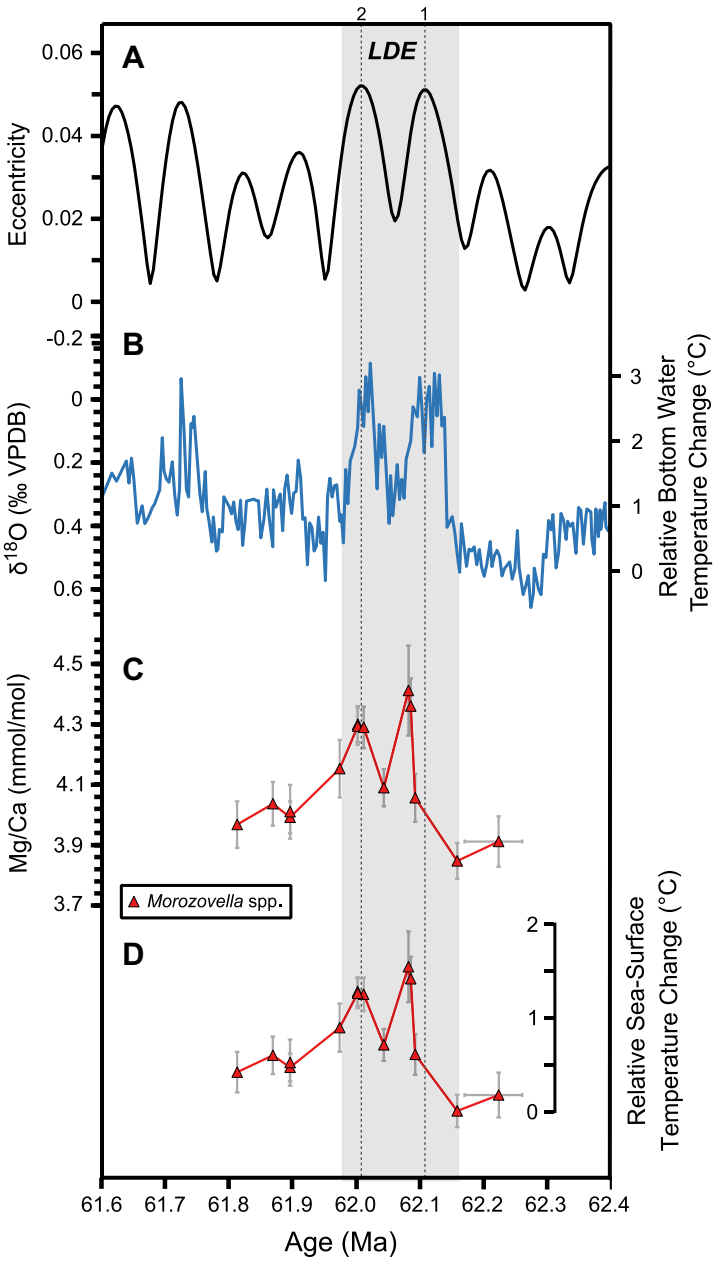


Figure 2: Relative changes in ocean temperature across the LDE at ODP Site 1262. Dashed vertical lines indicate the two benthic δ13C excursions forced by two 100-kyr eccentricity maxima, whilst the vertical grey bar encompasses the LDE as a whole. A: La2010b orbital solution of Laskar et al. (2011), labelled with the LDE interval. B: Benthic foraminiferal δ18O record (Barnet et al., 2019), plotted on an inverted scale. C: Planktic Mg/Ca ratios of Morozovella spp. (this study). D: Mg/Ca-derived relative change in sea surface temperature (this study). Error bars on the temperature data points represent average propagated analytical uncertainty from the Mg/Ca data.

1B), indicating pulsed decreases in deep ocean carbonate ion concentration during both LDE1 and LDE2. This suggests that the minima in $CaCO_3$ content at these times (Figures 1C, 3D) are indicative of carbonate dissolution events (Jehle et al., 2015, 2019).

## Surface Ocean Acidification

Within our planktic B/Ca data, we observe notable changes in surface ocean carbonate chemistry, broadly consistent with input of isotopically light carbon and resulting acidification. Since the ~200 kyr duration of the LDE is short compared to the residence times of boron (~10 Myr) and calcium (~1 Myr) within the ocean (Broecker & Peng, 1982; Lemarchand et al., 2000), decreases in the $[B(OH)_4^-]$/DIC ratio suggest a decrease in seawater borate concentrations, due to a decrease in pH (which decreases the abundance of $[B(OH)_4^-]$ relative to $[B(OH)_3]$), and/or an increase in DIC. As with planktic Mg/Ca data, the initial drop in planktic B/Ca lags the onset of LDE1, which may be due to sediment reworking or other competing influences.

## Carbon injection, calcifiers, and the carbonate pump

The coupled, double-spiked negative carbon isotope, $\%CaCO_3$, and B/Ca excursions of the LDE are likely forced by an orbitally paced injection of isotopically-depleted carbon to the ocean-atmosphere system, similar to other later hyperthermal events (e.g. Zachos et al., 2010; Barnet et al., 2019). However, there are also some notable differences in the structure of B/Ca, in particular in planktics, compared to $\delta^{13}C$, suggestive of additional influences. Most notably, the ocean remains in a more acidic state following the LDE, even after recovery in $\delta^{13}C$ and $\%CaCO_3$. Indeed, despite the more corrosive conditions indicated by the decrease in benthic B/Ca, $\%CaCO_3$ recovers to higher values following the LDE, as does %Coarse Fraction, which increases by a factor of two (Figure 3C and Jehle et al., 2019), suggesting a striking increase in the mass of planktic foraminifera reaching the seafloor. This may be linked to a change in planktic foraminiferal assemblages across the LDE, with a shift from praemuricates to more heavily calcified morozovellids (Bornemann et al., 2021). A similar signal is seen in calcareous nannoplankton, which show a substantial increase in cell volume following the LDE (Figure 3A; Alvarez et al, 2019). Together, these data suggest an increase in the flux of $CaCO_3$ from surface waters into sediments, coincident with a shift to

more acidic conditions in both surface and deep waters.

As pelagic $CaCO_3$ burial is a major sink of ocean alkalinity, we suggest that these signals may be linked, with increased $CaCO_3$ burial causing an increase in alkalinity removal, resulting in more acidic conditions. The apparent increase in carbonate export across the LDE is somewhat unexpected, as carbon injection and more acidic conditions might be expected to result in a decrease in calcification efficiency (e.g. Henehan et al., 2017). However, we note a diversity of pelagic calcifier responses to acidification has been found experimentally (e.g. Ridgwell et al., 2017) and that recent work shows an increase in foraminiferal carbonate accumulation also occurs over the PETM (Barrett et al., 2023). Several mechanisms may contribute to an increase in carbonate export in response to hyperthermal warming. Firstly, these events may lead to a selective pressure for more robust, heavily calcified species and/or an expansion of the geographical range of larger, more heavily calcified tropical species, which may also grow more quickly in warmer waters (Barrett et al., 2023). Secondly, while the onset of these carbon injection events may have been associated with a decrease in carbonate saturation state, on the >100 kyr timescale of event recovery, the addition of carbon, in combination with enhanced silicate weathering, may result in an increase in saturation due to higher overall DIC, even if more acidic conditions persist (Hönisch et al., 2012). We thus highlight the potential for a novel biogeochemical/evolutionary feedback (similar to that proposed by McClelland et al., 2016), whereby carbon input promotes a shift to more heavily calcified species, enhancing the ocean alkalinity sink, and leading to a shift to a more acidic, $CO_2$-rich ocean-atmosphere state.

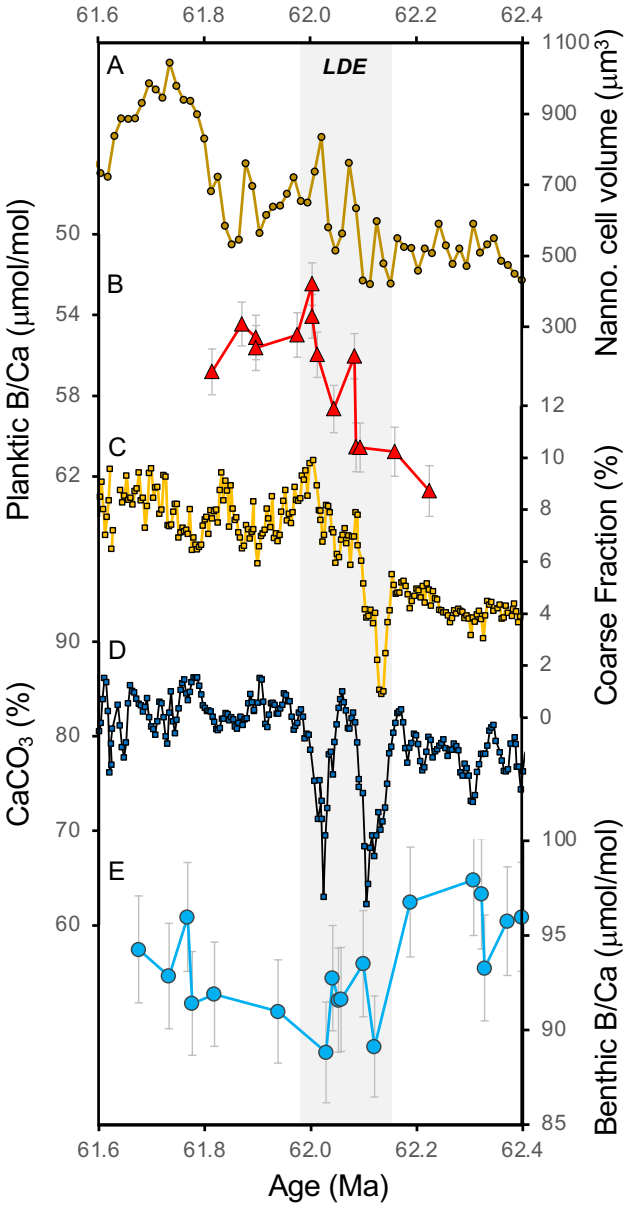


Figure 3: Evolution of the carbonate pump across the LDE. A: Cell volume of calcareous nannoplankton (Alvarez et al., 2021). B: Planktic B/Ca ratios of Morozovella spp. (this study). C: %Coarse Fraction (this study). D: %CaCO3 (Kroon et al., 2007). E: Benthic B/Ca ratios of N. truempyi (this study).

## CONCLUSIONS

Our new, paired foraminiferal B/Ca and Mg/Ca data show a clear response to a sudden release of isotopically light carbon to the ocean-atmosphere system during the LDE. The observed drops in benthic B/Ca, synchronous with negative excursions in benthic $\delta^{13}C$, suggest that carbon input drove ocean acidification and deep sea carbonate dissolution. Pulsed acidification and warming of the surface ocean are also evident from our planktic trace element records. Acidification persists following the LDE, which may be linked to an enhanced ocean alkalinity sink, due to a shift to more heavily calcified species of planktic foraminifera and larger calcareous nannoplankton,

suggesting a feedback between carbon cycle perturbation, calcification, and ocean-atmosphere $CO_2$.

## ACKNOWLEDGEMENTS

The complete trace element data set is available online in the PANGAEA database (https://doi.org/10.1594/PANGAEA.960288). Laboratory work was funded by a European Research Council grant awarded to James W.B. Rae (grant agreement 805246). We would like to thank Elizabeth Maerz for her help picking *S. beccariiformis*, as well as Kate Littler and an anonymous reviewer for their constructive comments and insight.

This publication is dedicated to the late Prof. Dick Kroon, without whom this manuscript would not have been possible. Dick's enthusiasm and contributions to paleoceanography, scientific ocean drilling, and the IODP will be his legacy, a paleo record which will live on into the future.

1

## REFERENCES CITED

Alegret, L., Ortiz, S., Arreguín-Rodríguez, G.J., Monechi, S., Millán, I., and Molina, E., 2016, Microfossil turnover across the uppermost Danian at Caravaca, Spain: Paleoenvironmental inferences and identification of the latest Danian event: Palaeogeography, Palaeoclimatology, Palaeoecology, v. 463, p. 45–59, doi:10.1016/j.palaeo.2016.09.013.

Alvarez, S.A., Gibbs, S.J., Bown, P.R., Kim, H., Sheward, R.M., and Ridgwell, A., 2019, Diversity decoupled from ecosystem function and resilience during mass extinction recovery: Nature, v. 574, p. 242–245, doi:10.1038/s41586-019-1590-8.

Babila, T.L., Penman, D.E., Hönisch, B., Kelly, D.C., Bralower, T.J., Rosenthal, Y., and Zachos, J.C., 2018, Capturing the global signature of surface ocean acidification during the Palaeocene–Eocene Thermal Maximum: Philosophical Transactions of the Royal Society A: Mathematical, Physical and Engineering Sciences, v. 376, p. 20170072, doi:10.1098/rsta.2017.0072.

Barrett, Ruby, Monsuru Adebowale, Heather Birch, Jamie D. Wilson, and Daniela N. Schmidt, 2023, Planktic Foraminiferal Resilience to Environmental Change Associated with the PETM: Paleoceanography and Paleoclimatology, v. 38, doi:10.1029/2022PA004534.

Barnet, J.S.K. et al., 2020, Coupled evolution of temperature and carbonate chemistry during the Paleocene–Eocene; new trace element records from the low latitude Indian Ocean: Earth and Planetary Science Letters, v. 545, p. 116414, doi:10.1016/j.epsl.2020.116414.

Barnet, J.S.K., Littler, K., Westerhold, T., Kroon, D., Leng, M.J., Bailey, I., Röhl, U., and Zachos, J.C., 2019, A High-Fidelity Benthic Stable Isotope Record of Late Cretaceous–Early Eocene Climate Change and Carbon-Cycling: Paleoceanography and Paleoclimatology, v. 34, p. 672–691, doi:10.1029/2019PA003556.

Bornemann, A., Schulte, P., Sprong, J., Steurbaut, E., Youssef, M., and Speijer, R.P., 2009, Latest Danian carbon isotope anomaly and associated environmental change in the southern Tethys (Nile Basin, Egypt): Journal of the Geological Society, v. 166, p. 1135–1142, doi:10.1144/0016-76492008-104.

Bornemann, A., Jehle, S., Lägel, F., Deprez, A., Petrizzo, M.R., and Speijer, R.P., 2021, Planktic Foraminiferal Response to an Early Paleocene Transient Warming Event and Biostratigraphic Implications: International Journal of Earth Sciences, v. 110, p. 583–594. doi:10.1007/s00531-020-01972-z.

Broecker, W.S., Peng, T., 1982, Tracers In The Sea: Radiocarbon, v. 24, p. B1-B2, doi:10.1017/S0033822200005221.

Brown, R.E., Anderson, L.D., Thomas, E., and Zachos, J.C., 2011, A core-top calibration of B/Ca in the benthic foraminifers Nuttallides umbonifera and Oridorsalis umbonatus: A proxy for Cenozoic bottom water carbonate saturation: Earth and Planetary Science Letters, v. 310, p. 360–368, doi:10.1016/j.epsl.2011.08.023.

Deprez, A., Jehle, S., Bornemann, A., and Speijer, R.P., 2016, Differential response at the seafloor during Palaeocene and Eocene ocean warming events at Walvis Ridge, Atlantic Ocean (ODP Site 1262): Terra Nova, v. 29, p. 71–76, doi:10.1111/ter.12250.

Evans, D. et al., 2018, Eocene greenhouse climate revealed by coupled clumped isotope-Mg/Ca thermometry: Proceedings of the National Academy of Sciences of the United States of America, v. 115, p. 1174–1179, doi:10.1073/pnas.1714744115.

Gothmann, A.M., Stolarski, J., Adkins, J.F., Schoene, B., Dennis, K.J., Schrag, D.P., Mazur, M., and Bender, M.L., 2015, Fossil corals as an archive of secular variations in seawater chemistry since the Mesozoic: Geochimica et Cosmochimica Acta, v. 160, p. 188–208, doi:10.1016/j.gca.2015.03.018.

Haynes, L.L., and Hönisch, B., 2020, The seawater carbon inventory at the Paleocene-Eocene Thermal Maximum: Proceedings of the National Academy of Sciences of the United States of America, v. 117, p. 24088–24095, doi:10.1073/pnas.2003197117.

Haynes, L.L., Hönisch, B., Holland, K., Rosenthal, Y., and Eggins, S.M., 2019, Evaluating the planktic foraminiferal B/Ca proxy for application to deep time paleoceanography: Earth and Planetary Science Letters, v. 528, p. 115824, doi:10.1016/j.epsl.2019.115824.

Henehan, M.J., Evans, D., Shankle, M., Burke, J.E., Foster, G.L., Anagnostou, E., Chalk, T.B., Stewart, J.A., Alt, C.H.S., Durrant, J., and Hull, P.M., 2017, Size-dependent response of foraminiferal calcification to seawater carbonate chemistry: Biogeosciences, v. 14, p. 3287–3308, doi:10.5194/bg-14-3287-2017.

Henehan, M.J. et al., 2019, Rapid ocean acidification and protracted Earth system recovery followed the end-Cretaceous Chicxulub impact: Proceedings of the National Academy of Sciences, v. 116,

p. 22500–22504, doi:10.1073/pnas.1905989116.

Hollis, C.J. et al., 2019, The DeepMIP contribution to PMIP4: Methodologies for selection, compilation and analysis of latest Paleocene and early Eocene climate proxy data, incorporating version 0.1 of the DeepMIP database: Geoscientific Model Development, v. 12, p. 3149–3206, doi:10.5194/gmd-12-3149-2019.

Hönisch, B. et al., 2012, The Geological Record of Ocean Acidification: Science, v. 335, p. 1058–1063, doi:10.1126/science.1208277.

Inglis, G.N. et al., 2020, Global mean surface temperature and climate sensitivity of the EECO, PETM and latest Paleocene: Climate of The Past Discussions, v. 44, p. 1–43, doi:10.31223/osf.io/8527z.

Jehle, S., Bornemann, A., Deprez, A., and Speijer, R.P., 2015, The Impact of the Latest Danian Event on Planktic Foraminiferal Faunas at ODP Site 1210 (Shatsky Rise, Pacific Ocean): PLoS ONE, v. 10, p. e0141644, doi:10.1371/journal.pone.0141644.

Jehle, S., Bornemann, A., Lägel, A.F., Deprez, A., and Speijer, R.P., 2019, Paleoceanographic changes across the Latest Danian Event in the South Atlantic Ocean and planktic foraminiferal response: Palaeogeography, Palaeoclimatology, Palaeoecology, v. 525, p. 1–13, doi:10.1016/j.palaeo.2019.03.024.

Kender, S., Yu, J., and Peck, V.L., 2014, Deep ocean carbonate ion increase during mid Miocene CO2 decline: Scientific Reports, v. 4, p. 1–6, doi:10.1038/srep04187.

Kroon, D., Zachos, J.C., and Leg 208 Scientific Party, 2007, Leg 208 synthesis: Cenozoic climate cycles and excursions: Proceedings of the Ocean Drilling Program: Scientific Results, v. 208, doi:10.2973/odp.proc.sr.208.201.2007.

Laskar, J., Fienga, A., Gastineau, M., and Manche, H., 2011, La2010: A new orbital solution for the long-term motion of the Earth: Astronomy and Astrophysics, v. 532, doi:10.1051/0004-6361/201116836.

Lemarchand, D., Gaillardet, J., Lewin, and Allégre, C.J., 2000, The influence of rivers on marine boron isotopes and implications for reconstructing past ocean pH: Nature, v. 408, p. 951–954, doi:10.1038/35050058.

McClelland, H.L.O., Barbarin, N., Beaufort, L., Hermoso, M., Ferretti, P., Greaves, M., Rickaby, R.E.M., 2016, Calcification response of a key phytoplankton family to millennial-scale environmental change: Sci Rep, v. 6, doi:10.1038/srep34263.

Rae, J.W.B., Zhang, Y.G., Liu, X., Foster, G.L., Stoll, H.M., Whiteford, R.D.M., 2021, Atmospheric $CO_2$ over the past 66 million years from marine archives: Annual Review of Earth and Planetary Sciences, doi:10.1146/annurev-earth-082420-063026.

Ridgwell, A., Schmidt, D.N., Turley, C., Brownlee, C., Maldonado, M.T., Tortell, P., Young, J.R., 2009, From laboratory manipulations to Earth system models: scaling calcification impacts of ocean acidification: Biogeosciences, v. 6, p. 2611–2623, doi:10.5194/bg-6-2611-2009.

Westerhold, T., Rhl, U., Donner, B., McCarren, H.K., and Zachos, J.C., 2011, A complete high-resolution Paleocene benthic stable isotope record for the central Pacific (ODP Site 1209): Paleoceanography, v. 26, p. 1–13, doi:10.1029/2010PA002092.

Westerhold, T., Röhl, U., Raffi, I., Fornaciari, E., Monechi, S., Reale, V., Bowles, J., and Evans, H.F., 2008, Astronomical calibration of the Paleocene time: Palaeogeography, Palaeoclimatology, Palaeoecology, v. 257, p. 377–403, doi:10.1016/j.palaeo.2007.09.016.

Zachos, J.C., Kroon, D., Blum, P., and Party, S.S., 2004, Site 1262: Proceedings of the Ocean Drilling Program, Initial Reports, v. 208, doi:10.2973/odp.proc.ir.208.103.2004.

Zachos, J.C., McCarren, H., Murphy, B., Röhl, U., and Westerhold, T., 2010, Tempo and scale of late Paleocene and early Eocene carbon isotope cycles: Implications for the origin of hyperthermals: Earth and Planetary Science Letters, v. 299, p. 242–249, doi:10.1016/j.epsl.2010.09.004.

Zeebe, R.E., and Tyrrell, T., 2019, History of carbonate ion concentration over the last 100 million years II: Revised calculations and new data: Geochimica et Cosmochimica Acta, v. 257, p. 373–392, doi:10.1016/j.gca.2019.02.041.